*3rd Micro and Nano Flows Conference*
*Thessaloniki, Greece, 22-24 August 2011*

# Boundary Condition, An Old But Not Well Solved Problem, Linked From Nanometer To Macroscale

Jinliang XU[1,2], Yuxiu LI[3]

*Corresponding author: Tel.:++86(10)61772268; Fax: ++86(10)61772268; Email: xjl@ncepu.edu.cn
1: State Key Laboratory of Alternate Electrical Power System with Renewable Energy Sources, North China Electric Power University, Beijing 102206, China
2: The Beijing Key Laboratory of New and Renewable Energy, North China Electric Power University, Beijing, 102206, P.R. China
3: Guangzhou Institute of Energy Conversion, Guangzhou, 510640, P.R. China

**Abstract** A key issue of the flow and heat transfer in channels is to determine the boundary condition, which is affected by various parameters, such as the solid-fluid potential interactions, solid wall roughness, surface wettability etc. We summarize the progress that has been made in recent years. In the first part of this paper, we reviewed the three-atom-model, leading to an important criterion number governing the boundary conditions. The molecular dynamics (MD) simulations verified the effectiveness of the criterion number. The second part of this paper reports the multiscale simulation of the flow field in channels, adjoining the molecular dynamics (MD) simulation and the continuum fluid mechanics. Three types of boundary conditions (slip, non-slip and locking) were identified over the multiscale channel sizes. The slip lengths are found to be mainly dependent on the interfacial parameters with the fixed apparent shear rate. The channel size has little effects on the slip lengths if the size is above a critical value within a couple of tens of molecular diameters. The slip, non-slip and locking interfacial parameters yield positive, zero and negative slip lengths, respectively. The three types of boundary conditions existing in "microscale" still occur in "macroscale". However, the weak dependence of the slip lengths on the channel size yields decreased slip velocities with increases in channel sizes for all three types of interfacial parameters.

**Keywords**: boundary condition, molecular dynamics, multiscale, slip length

## 1. Introduction

The boundary condition (BC) is an old but not a well solved problem, which is important in confined flow system, such as in porous media, microfluidic devices, fluid lubrication system, biology system, etc. The BC problem has been received attention since the 18th century. Two viewpoints: no-slip BC, or slip BC, have been proposed, which have competed with each other. But the no-slip BC has been widely used in scientific history. Many great scientists have commented on the BC problem And the main points about it over the 18th to 20th century period are summarized as follows.

**The no-slip BC:** The early experimenters did not observe fluid slip at the solid wall surface. Bernoulli[1] proposed that fluid at the solid wall surface has the same velocity as that of the solid wall, but the fluid velocity increases with distance from the solid wall, for the first time. Stokes[2] and Buat[3] postulated that the water near a wall surface is stationary when the average flow velocity of water is smaller than a specific value. Coulomb[4] concluded that fluid molecules on a vibrating solid cylinder wall have the same

velocity as that of the solid cylinder. The fluid velocity is small from a small distance from the cylinder, but the velocity decreases to almost zero for the distance of several millimeters away from the solid cylinder.

**The stationary layer BC:** It is assumed that there is a thin liquid layer adhering to the solid wall. The liquid layer is stationary with respect to the solid wall. The liquid above the thin stationary liquid layer slipps over the stationary liquid layer.

**The local BC:** Navier[5] proposed that liquids can slip on the solid wall surface. But the frictional force prevents motion due to the slip motion. The frictional force is proportional to the fluid velocity relative to the solid wall. He proposed the slip length concept to quantify the slip degree, which has been used up to now. He related that the slip length to the slip velocity at the solid-liquid interface by:

$$L_s = b\frac{\partial u_b}{\partial z} \quad (1)$$

where $u_b$ is the streamline velocity, $z$ is the coordinate perpendicular to the solid wall surface.

Researchers began to consider the physical mechanism of the boundary condition problem from the 1930s. Stokes[2] recommended the combination of the two types of boundary conditions: a stationary fluid layer adhering to the wall surface, and an additional layer above stationary layer to satisfy the boundary condition proposed by Navier. Stokes[2] studied the physical mechanism of the boundary condition in the 1940s. His computational results disagreed with the experimental data. But finally he decided to accept the no-slip boundary condition assumption.

Poiseuille[6] reported a stationary fluid layer for blood flowing in a tube. He observed the flow in a glass tube with opaque particles suspended in liquids, and identified the existence of a stationary layer. Such a flow in a capillary tube is termed Poiseuille flow. Helmholtz and Piotrowski[7] postulated that the fluid velocity at the wall surface is not always the same as that of the solid wall, but that a slip velocity exists at the wall surface. They charged different working liquids in a vibrating glass container. They did not find a slip BC when water or methanol liquid charge in the glass beaker. However, apparent slip BC appeared when water is insider the glass beaker surfaced with a gold pattern. Maxwell[8] dismissed these experimental results, due to the poor measurement accuracy which was not sufficient to quantify the small slip length. Even though considered efforts was made, there was no general conclusion on the BC problem at that time.

From then on the no-slip BC assumption was used widely. Whetham[9] performed experiments with water flowing in silver or copper tubes with a minimum tube diameter of 1.0 mm, but did not find the slip phenomenon. Couette[10], Maxwell[11], and Ladenburg[12] reached a similar conclusion independently. In the 20$^{th}$ century researchers deceived that the slip length is too small to be detected even though the phenomenon existed. At the middle of the 20$^{th}$ century, general agreement had still not been reached about the BC problem, and scientists and engineers widely used the no-slip BC. At the end of the 20$^{th}$ century, due to the miniaturization and development of micro/nano scale machines, the BC problem has received great attention. This was because the boundary condition has a significant effect on the flow and heat transfer in micro/nano scale channels.

Various factors influence the boundary conditions. These include the molecular potential interactions between the solid wall

and a fluid, solid wall surface roughness, surface wettability and nano-bubbles entrapped in small cavities of wall surface. While a thorough review of the BC problem is beyond the scope of this paper, in the first part, we discuss the three-atom-model at the solid-liquid interface. This leads an important criterion number which governs the boundary conditions at the wall surface. The criterion number is verified by molecular dynamics simulations. In the second part of the paper, we demonstrate a multiscale approach to compute Couette flow. We were able to repeat the three types of boundary conditions. We found that the slip lengths are mainly dependent on the interfacial parameters, while the channel size has little effect on the boundary conditions.

## 2. The three-atom-model

### 2.1 Presentation of the model[13]

There are many factors influencing the boundary conditions,but here we mainly consider the effect of molecular interactions.. The following assumptions are made: (1) solid wall atoms are arranged in the fcc structure; (2) there is a liquid argon atom on the plane of the solid wall.

We consider the liquid argon with a non-dimensional density of $\rho\sigma^3 = 0.81$ , where $\rho$ is the liquid atom density and $\sigma$ is the length scale. The length of a unit lattice cell for the liquid argon assuming a fcc structure leads to $L_{\text{argon}}$=1.7σ. The Lennard-Jones potential for a pair of liquid argon atoms is written as

$$\phi_{l-l} = 4\varepsilon\left[\left(\frac{\sigma}{r}\right)^{12} - \left(\frac{\sigma}{r}\right)^{6}\right] \quad (2)$$

where $\varepsilon$ is the energy scale, $r$ is the distance between a pair of liquid atoms.

When the LJ potential, Eq.2, is used for the interactions between solid and liquid atoms, the coupling energy scale $\varepsilon_{wf}$ and the length scale $\sigma_{wf}$ of the solid/liquid interactions are used instead. Defining $C_2=\varepsilon_{wf}/\varepsilon$ and $C_3=\sigma_{wf}/\sigma$, the pair potential is changed to be

$$\phi_{l-s} = 4C_2\varepsilon\left[C_3^{12}\left(\frac{\sigma}{r}\right)^{12} - C_3^{6}\left(\frac{\sigma}{r}\right)^{6}\right] \quad (3)$$

Using the non-dimensional length, $r^*=r/\sigma$, the non-dimensional potential is written as

$$\frac{\phi_{l-s}}{\varepsilon} = 4C_2\left(\frac{C_3^{12}}{r^{*12}} - \frac{C_3^{6}}{r^{*6}}\right) \quad (4)$$

Using $F = -\dfrac{\partial\phi}{\partial r}$, the force between a pair of solid and liquid atoms in non-dimensional unit yields

$$F^* = \frac{F\sigma}{\varepsilon} = 24C_2\left(\frac{2C_3^{12}}{r^{*13}} - \frac{C_3^{6}}{r^{*7}}\right) \quad (5)$$

We assign the particle density of the solid atoms as $\rho_w$ and define the density ratio relative of the solid to the liquid as $C_1=\rho_w/\rho$. Thus the length of a unit lattice cell for the solid wall is

$$L = 1.7\sigma C_1^{-1/3} \quad (6)$$

From Eqs.5~6 it is seen that the liquid movement at the solid/liquid interface is governed by the three non-dimensional parameters of $C_1$, $C_2$ and $C_3$.

A random unit lattice cell at the first layer of the solid wall is selected, with the four solid atoms marked as A, F, B and E (see Fig.1). The liquid atom $C$ is located on the line between A and B, at which a local coordinate $x$ is attached (one-dimensional coordinate). The atoms A and B have the coordinates of $(-0.85C_1^{-1/3})$ and $(0.85C_1^{-1/3})$, scaled by $\sigma$.

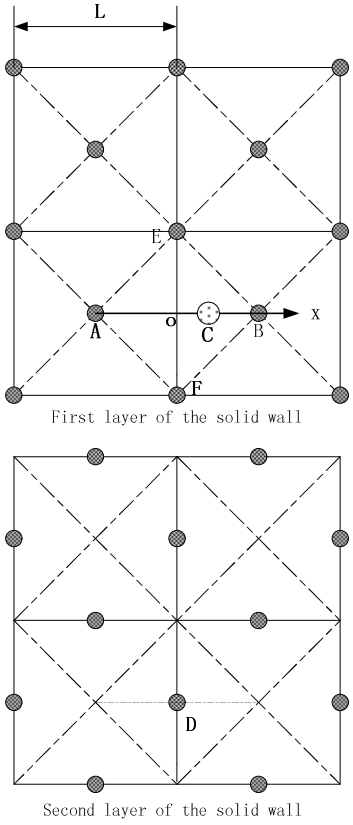


*Fig.1 The first and second layer of the solid walls based on the fcc structure*

A zero force is achieved between the liquid atom C and the four neighboring solid atoms of A, F, B and E if the liquid atom *C* is located at *x*=0. If the liquid atom *C* is located in the range of $0 < x < 0.85C_1^{-1/3}$, $F_{B-C}$ is the largest one for the force interactions between the liquid atom C and the four neighboring solid atoms, due to the short distance force behavior for the molecular interactions. Similarly if the liquid atom C is in the range of $-0.85C_1^{-1/3} < x < 0$, $F_{A-C}$ contributes the major part. Therefore, when the liquid atom *C* is traveling on the line AB, only two forces of $F_{A-C}$ and $F_{B-C}$ are needed to be considered. The potentials $\phi_{A-C}+\phi_{B-C}$ and forces $F_{A-C}+F_{B-C}$ are written as

$$\frac{\phi_{A-C}+\phi_{B-C}}{\varepsilon} = \underbrace{4C_2\left[\frac{C_3^{12}}{(0.85C_1^{-1/3}+x)^{12}}-\frac{C_3^{6}}{(0.85C_1^{-1/3}+x)^{6}}\right]}_{\frac{\phi_{A-C}}{\varepsilon}} + \underbrace{4C_2\left[\frac{C_3^{12}}{(0.85C_1^{-1/3}-x)^{12}}-\frac{C_3^{6}}{(0.85C_1^{-1/3}-x)^{6}}\right]}_{\frac{\phi_{B-C}}{\varepsilon}} \quad (7)$$

$$\frac{(F_{A-C}+F_{B-C})\sigma}{\varepsilon} = \underbrace{24C_2\left[\frac{2C_3^{12}}{(0.85C_1^{-1/3}+x)^{13}}-\frac{C_3^{6}}{(0.85C_1^{-1/3}+x)^{7}}\right]}_{\frac{F_{A-C}\sigma}{\varepsilon}} - \underbrace{24C_2\left[\frac{2C_3^{12}}{(0.85C_1^{-1/3}-x)^{13}}-\frac{C_3^{6}}{(0.85C_1^{-1/3}-x)^{7}}\right]}_{\frac{F_{B-C}\sigma}{\varepsilon}} \quad (8)$$

Eqs.7~8 relate the liquid atom C with the two solid atoms of A and B, thus the "three-atom-model" is named. Here we temporarily introduce a new parameter of $\lambda = C_1^{1/3}C_3$. It is seen from Fig.2 that there are two minimal points of potential corresponding to the two zero forces, marked at *I* and *J*. The left and right zero force points are calculated at $x_I = 2^{1/6}C_3 - 0.85C_1^{-1/3}$ and $x_J = -2^{1/6}C_3 + 0.85C_1^{-1/3}$, respectively. Thus the length *IJ* is

$$L_{IJ} = x_J - x_I = 2(0.85C_1^{-1/3} - 2^{1/6}C_3) \quad (9)$$

Note that $x_I$, $x_J$ and $L_{IJ}$ in Eq.9 are scaled by $\sigma$. We define three regions along the line of AB (see Fig.2).

(1) **The high repulsive force region (** $-0.85C_1^{-1/3} < x < x_I$ **and** $x_J < x < 0.85C_1^{-1/3}$**)**. High repulsive force in this region prevents the liquid atoms populating there.

(2) **The liquid atom metastable region (** $x_I < x < x_P$ **and** $x_Q < x < x_J$ **)**. We define two other points of *P* and *Q* at which the forces are very close to zero. If the liquid atom C is in this region, the attractive force from the solid atom A or B extracts the liquid atom C toward the

solid atoms of A or B. However, when the atom C reaches at $x_I$ or $x_J$, the high repulsive force pushes the atom *C* back to the region of $x_I < x < x_P$ **or** $x_Q < x < x_J$. Thus the **li**quid atom *C* in these regions are in a metastable state.

**(3) The liquid atom free population region** ($x_P < x < x_Q$) The force in this region is very close to zero, liquid atoms are being freely populated there. A liquid atom cannot follow the motion of the solid atoms of *A* and *B*.

Referring to Fig.2, we define η as the length of *IJ* with respect to *AB* as

$$\eta = \frac{L_{IJ}}{L_{AB}} = \frac{2(0.85C_1^{-1/3} - 2^{1/6}C_3)}{1.7C_1^{-1/3}} = 1 - 1.32C_1^{1/3}C_3 \quad (10)$$

We further define the important criterion number of λ as $C_1^{1/3}C_3$. η is zero if λ equals to 0.757, corresponding to the two zero force points shrinking to one point at $x$=0. Physically, λ=0.757 indicates that the liquid atom will exactly follow the motion of the solid atoms, inferring the no-slip boundary condition, or the locking boundary condition. Considering Fig.2, it is found that the liquid freely populated region will be enlarged with decreases in λ if λ<0.757. In other words, the slip degree shall be enhanced with decreases in λ.

Now we consider the situation of λ>0.757. As shown in Fig.2b, if $\lambda$ is larger than 0.757, such as $\lambda = 1.0$, the potential and force curves show similar shapes as those at λ=0.757. However, the $F_{A-C} + F_{B-C}$ force curve has a very steep gradient near $x$=0. It seems that the no-slip or locking BCs is enhanced with increases in λ for λ>0.757. However, our MD simulation does not support this conclusion. In fact the slip BC phenomenon takes place under such circumstance. This is due to the force interaction between the liquid atom C and the solid atom *D* of the second layer (see Fig.1). In terms of the fcc structure of the solid walls, the solid atom *D* is just below the central point of the line *AB* by $0.5L$ in the vertical plane (*xz* plane). In summary, the no-slip BC or locking BC is enhanced when λ equals to 0.757. Deviation of λ from 0.757 yields slip boundary conditions. $C_2$ also influences the boundary conditions. Figure 3 shows three groups of curves, with $\lambda = 0.2$, 0.5 and 0.76 respectively. There are three curves in each group, each corresponding to $C_2 = 0.2$, 1.0 and 4.0 respectively. For a specific $\lambda$, larger $C_2$ leads to a higher attractive force, inducing more liquid particles to populate the region of IP, causing the decreased slip degree.

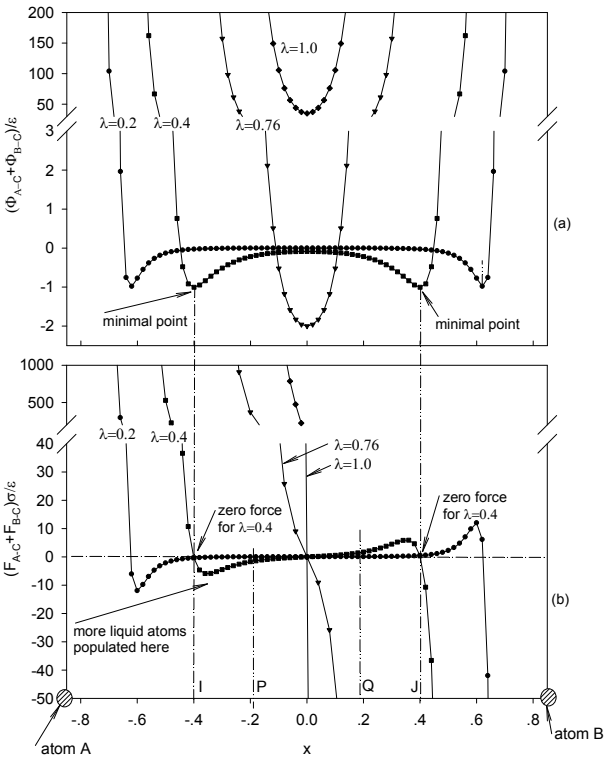


*Fig.2 Potential and force between the liquid atom and the two solid atoms at the interface* ($C_1 = 1.0, C_2 = 1.0$)

## 2.2 Verification by molecular dynamics simulations

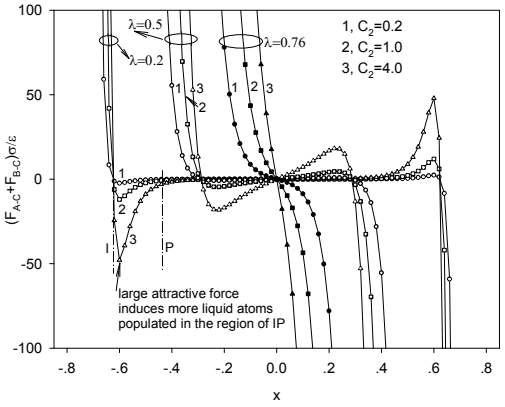


*Fig.3 Combined effect of $\lambda$ and $C_2$ on the force between the liquid atom and the two solid atoms ($C_1 = 1.0$)*

Molecular dynamics (MD) simulations were performed for a Couette flow geometry, with $N$=864 liquid atoms included in the cubic structure, corresponding to a cubic arrangement of $L_x$=$L_y$=$L_z$=10.22σ for the liquid calculation domain. The top and bottom solid atoms depend on $C_1$ and $C_3$. For instance, there are $N_{w,top}$=$N_{w,bottom}$=294 solid particles for $C_1$=1.0 and $C_3$=0.8. However, there are $N_{w,top}$=$N_{w,bottom}$=800 solid atoms for $C_1$=4.63, and $C_3$=1.0.

Intermolecular forces are considered not only among liquid atoms, but also between liquid atoms and solid walls, are considered. Periodic boundary conditions are applied in $x$ and $y$ coordinates outside of the calculation domain. At the start-up of the MD simulations, initial conditions are set for liquid particle locations, velocities and higher order derivatives. Initial positions of liquids are set as fcc structure, which will melt after the MD simulations are performed. Random initial velocities of liquid particles are assumed, but scaled by the liquid temperatures by $T_B$=1.1$k_B$/ε. The initial particle accelerations are decided based on the positions of $r_i(0)$ by computing the forces on each atom and applying Newton's second law. The initial higher order derivative is assumed to be zero, but will be updated following the MD simulations. The detailed computation process can be found in Ref. 13.

Figure 4 shows velocity profiles dependent on $\lambda$ and $C_2$. Figure 4a shows that when λ=0.8 which approaches 0.757, the flow approaches the no-slip or locking BCs. With increases in $C_2$ from 0.2 to 4.0, the flow switches from the quasi-no-slip BCs (velocity profiles dotted by "●" for $C_2 = 0.2$ and "■" for $C_2 = 0.6$) to the locking BCs (dotted by "▲" for $C_2 = 1.8$ and "▼" for $C_2 = 4.0$). For the locking BCs, the velocity profiles are not straight lines. Velocity gradients near the solid wall are very gentle for several liquid layers. Figure 4(b-c) shows velocity profiles for equal and unequal densities of solids and liquid systems, $C_1$=1.0 and $C_1$=4.63 both with $C_2$=0.6. Both subfigures in Fig.4(b-c) show that the flow approaches the no-slip BCs when λ approaches 0.757. Deviation of λ from 0.757 induces the increased slip degree. Figure 4 strongly support the three-atom–model theory.

## 3. The multiscale simulation of the BC problems[14]

MD simulations can only treat the computational domain at the nanoscale. When the channel size is further increased, an effective way is the hybrid method. Again we consider Couette flow sheared by two solid walls, which are traveling at constant speeds in opposite directions. Slip lengths and macroscopic velocity profiles are determined by the hybrid computation scheme. The following assumptions were made for the present multiscale simulations:

- Intermolecular force interactions are not only considered among liquid argon particles, but also between argon atoms and solid walls. Solid-liquid interactions have similar potentials as those among the liquid particles, leading to three

interfacial parameters given in the above section ($C_1$, $C_2$ and $C_3$).

- We specify the non-dimensional apparent shear rate of $\gamma_a\tau$=0.05, where $\gamma_a$ and $\tau$ are the apparent shear rate and the characteristic time of argon.

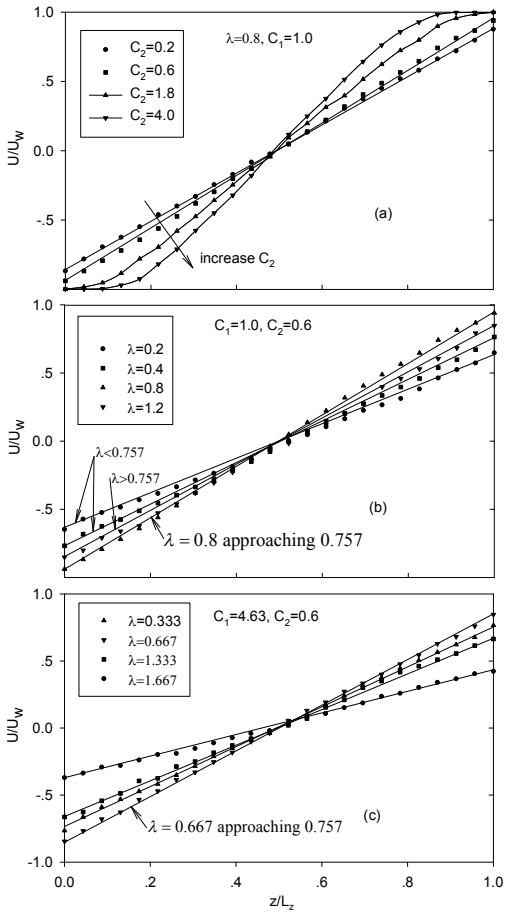


*Fig.4 Effect of $\lambda$ and $C_2$ on the velocity profiles for Couette flow.*

The scheme employs MD near the walls (the *P* region in Fig.5) where the molecular effects are important. Only a very thin layered fluid with a thickness of several times the cut-off distance of 2.5σ needs to be considered due to the short range intermolecular force characteristic among particles. Other regions apart from the thin fluid layer can be treated by continuum fluid mechanics (the *C* region in Fig.5). An overlap region is set in which both MD and continuum fluid mechanics are considered. Mass, momentum and energy exchanges take place there. Advantage of the hybrid approach is in the reduction of computation time for a large molecular number system. Besides, the method significantly extends the computational domain beyond the scope of the MD simulations.

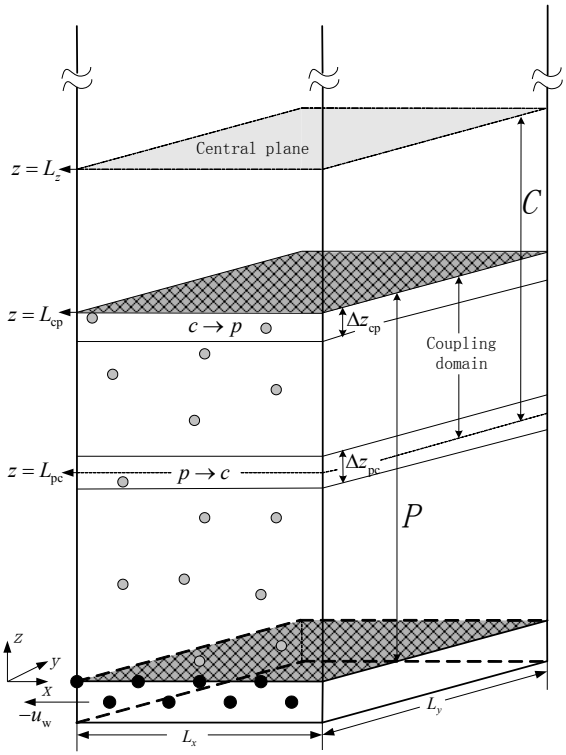


*Fig.5 The Couette flow geometry and the domain decomposition.*

Classical MD simulations are only suitable for a length scale of ten nanometers, but the length scale can be significantly extended by the hybrid computation scheme. This is quite useful when only a small amount of fluid needs to be considered at the scale of atoms but the fluid bulk is described by continuum fluid mechanics. Mass, momentum and energy exchanges in the $c \to p$ and $p \to c$ layers will be considered (see Fig.5).

***The $p \to c$ coupling*** Regarding Fig.5, it should be noted that the center plane of the Couette flow has zero mean axial velocity due to geometrical symmetry. The continuum fluid mechanics simulation in the $C$ domain needs a boundary condition of the mean axial

velocity at $z=L_{pc}$, which is from the $p \to c$ coupling. Assuming that the mean axial velocity $u_{p\to c}$ at $z = L_{pc}$ is known from the parameter averaging based on the MD simulations, the linear velocity profile over the $C$ domain is written as

$$u = -\frac{u_{p\to c}}{L_z - L_{pc}}(z - L_z) \quad (11)$$

Again, it should be noted that the linear velocity profile in the $C$ domain is ensured because the interface at $z=L_{pc}$ is so "far" that solid wall particles have no effect on liquid atoms in the $C$ domain.

***The*** $c \to p$ ***coupling*** MD simulations treat the bottom boundary by computing the intermolecular force interactions between liquid and solid atoms. We note that the MD simulations lack another boundary condition at $z=L_{cp}$, which can be from the $c \to p$ coupling.

From Eq. 11, the shear stress at the interface of $z=L_{cp}$, can be derived as

$$\tau = \mu \frac{\partial u}{\partial z} = -\mu \frac{u_{p\to c}}{L_z - L_{pc}} \quad (12)$$

The total shear force at the interface of $z=L_{cp}$ is

$$F_{ext} = \tau L_x L_y = -\mu \frac{u_{p\to c}}{L_z - L_{pc}} L_x L_y \quad (13)$$

Our previous study shows that the viscosity $\mu$ follows $\mu / \varepsilon\tau\sigma^{-3} = 2.0$ . We assume that such external force is applied uniformly on each liquid atom within the layer of $c \to p$, thus $F_{ext} / N_{cp}$ is the external force term in Eq.13, yielding the closure relation for the MD simulation over the entire $P$ domain.

Here we only consider the equal density system of solids and liquids, thus $C_1$=1.0. We select three groups of interfacial parameters as follows:

$$\left.\begin{aligned} C_1 = 1.0, C_2 = 0.2, C_3 = 0.3 \\ C_1 = 1.0, C_2 = 1.0, C_3 = 0.7 \\ C_1 = 1.0, C_2 = 4.0, C_3 = 0.76 \end{aligned}\right\} \quad (14)$$

The above parameters correspond to

$$\left.\begin{aligned} \lambda = 0.3, C_2 = 0.2 \\ \lambda = 0.7, C_2 = 1.0 \\ \lambda = 0.76, C_2 = 4.0 \end{aligned}\right\} \quad (15)$$

for the slip, no-slip and locking boundary conditions respectively. We name the three groups of parameters as the slip, no-slip and locking interfacial parameters, respectively.

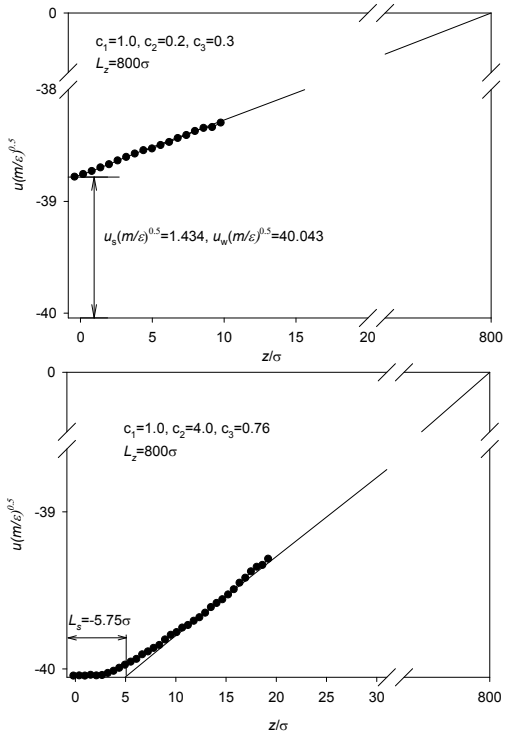


*Fig.6 The mean velocity profiles across the half channel height with $L_z$=800σ。*

Figure 6 shows mean axial velocity profile across the half channel height for the slip and locking BC interfacial parameters with $L_z$=800σ. Data points are only available in the $P$ domain. The linear velocity distribution followed by the $P$ domain is predicted by Eq.11. A perfect linear velocity profile is observed across the entire half channel height (see Fig.6a), with $u_w(m/\varepsilon)^{0.5} = 40.043$ and $u_s(m/\varepsilon)^{0.5} = 1.434$ for the slip interfacial parameter. A curved velocity distribution is

observed near the solid wall, followed by the linear distribution, for the locking BC. The slope at z=$L_z$ determines a slip length of $L_s$=-5.75σ.

Figure 7 shows slip lengths for the three interfacial parameters (see Eq.15) with $L_z$ from 5 to 3000σ, corresponding to 1.7 nm to 1.022 μm. It is shown that slip lengths do not change for a specific group of interfacial parameter, i.e., slip lengths are only dependent on interfacial parameters, not on channel size. A perfect zero slip length can be reached for the no-slip interfacial parameter of λ=0.7 and $C_2$=1.0 with $L_z$ from nano to micron. A slip interfacial parameter of λ=0.3, $C_2$=0.2 induces the slip length of 29.7σ=10.12 nm and the locking interfacial parameter of λ=0.76, $C_2$=4.0 results in the slip length of -5.7σ=−1.94 nm.

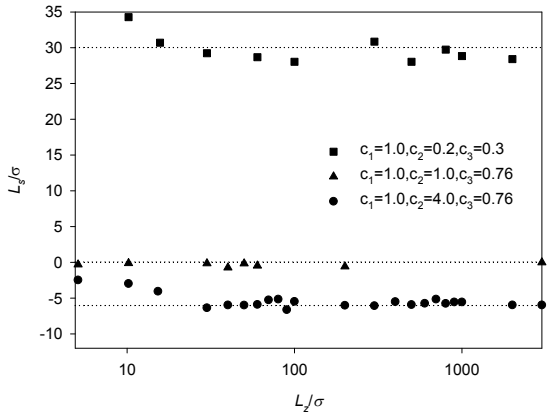


*Fig.7 Constant slip lengths versus channel size for the three typical interfacial parameters.*

Further, we plot $\gamma_r\tau$ and $u_s/u_w$ versus $L_z$ for the three typical interfacial parameters in Fig.8. It should be noted that $\gamma_r$ is the real shear rate at z=$L_z$. The no-slip interfacial parameter yields $\gamma_r \approx \gamma_a$ and $u_s \approx 0$ with $5\sigma \le L_z \le 3000\sigma$, where $\gamma_a$ is the apparent shear rate. For the slip interfacial parameter of $\lambda = 0.3, C_2 = 0.2$, the non-dimensional real shear rates of $\gamma_r\tau$ are smaller than the non-dimensional apparent shear rate of $\gamma_a\tau = 0.05$, but they are increased with increases in $L_z$. Meanwhile the slip velocity relative to the solid speed of $u_s/u_w$ decreases with increases in $L_z$. Both of $\gamma_a\tau$ and $u_s/u_w$ approach those for the no-slip solutions when $L_z$>1000σ. The locking interfacial parameter of $\lambda = 0.76, C_2 = 4.0$ yields real shear rates higher than the apparent value but they decrease with increases in $L_z$. Similar to the Couette flow for the slip interfacial parameter, $\gamma_r\tau$ and $u_s/u_w$ approach those for the no-slip BCs when $L_z$>1000σ.

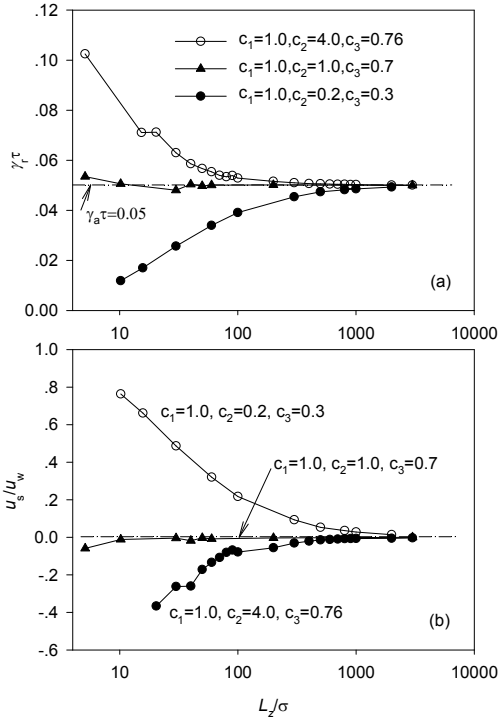


*Fig.8 Real shear rates and slip velocities relative to the solid wall speed versus channel size by the hybrid computations.*

The above finding helps us to identify the physical mechanisms of the boundary conditions. There is no transition from "micro" to "macro". The interfacial parameters govern the slip lengths, which are not dependent on the channel size. The three types of boundary conditions existing in "microscale" still occur in "macroscale". ***This is the absoluteness of the boundary conditions.*** Real shear rates and slip velocity relative to the solid wall speed approach those with the no-slip boundary condition

when the channel size is larger than thousands of molecular diameters for all the three types of interfacial parameters, leading to the quasi-no-slip boundary conditions. ***This is the relativity of the boundary conditions.***

## *4. Conclusions*

The boundary condition is an old but not a well understood problem. Many factors influence the boundary condition. This issue has become more important recently due to the development of miniature machines. Here we consider a simple run with a smooth wall surface. We propose a three-atom-model and develop a criterion number governing the boundary conditions. When the criterion number equals to 0.757, no-slip BC or locking BC occurs. Deviation of the criterion number from 0.757 induces the increased slip degree. The three-atom-theory is verified by the molecular dynamics simulations.

A multiscale scheme is proposed to compute the flow field in a Couette flow geometry, joining the molecular dynamics simulations and the continuum fluid mechanics. Three typical interfacial parameters are chosen. It is found that slip lengths are mainly dependent on the interfacial parameters, but only very weakly dependent on the channel size. ***This is the absoluteness of the boundary conditions.*** However, slip velocities relative to solid wall speed approach those with the no-slip boundary condition when the channel size is larger than thousands of molecular diameters for all the three types of interfacial parameters, leading to the quasi-no-slip boundary conditions. ***This is the relativity of the boundary conditions.***

## *Acknowledgements*

This work is supported by the National Natural Science Foundation of China (No. U1034004 and 50825603), and the Basic Research Program (973 program) with the contract number of 2011CB710703.

## *References:*

1. *Bernoulli D, Hydrodynamica, p 59,1783.*
2. *Stokes G G, On the Theories of the Internal Friction of Fluids in Motion, and of the Equilibrium and Motion of Elastic Solids Mathematical and Physical Papers by George Stokes (Cambridge: Cambridge University Press) vol 1, pp 75-187,1966.*
3. *Du Buat P L G, Principes d'Hydraulique p 92-3,1786.*
4. *Coulomb C A, Memoires de l'Institut National des Sciences et des Arts: Sciences Mathematiques et Physiques vol 3,1801.*
5. *Navier C L M H，Mem. Acad. Sci. Inst. Fr. 6 432-6，1823*
6. *Poiseuille J L M, Recherches Experimentales Sur Ie Mouvement Des Liquides Dans les Tubes de Tres Petits Diametres; IV. Influence de la Temperature Sur la Quantite de Liquide qui Traverse les Tubes de Tres Petits Diametres. C. R. Acad. Sci. 12, 112-15, 1841.*
7. *Helmholtz H and von Piotrowski G, "Ueber die Reibung Tropfbarer Flüssigkeiten," Sitzungsberichte der mathematisch-naturwissenschaftlichen Classe der k.k. Akademie der Wissenschaften zu Wien 40, 607–658, 1860.*
8. *Maxwell J C, Scientific Papers (Dover, New York), Vol. 2, p. 704, 1953*
9. *Whetham W C D, Phil. Trans. R. Soc. Lond. Ser. A, 181 559,1890*
10. *Couette M, Ann. Chim. Phys., 21, 433–510, 1890*
11. *Maxwell J C, The Scientific Papers of James Clerk Maxwell (Cambridge: Cambridge University Press), vol 2, pp 1–25, 1890*
12. *Ladenburg R, Ann. Phys., 4, 447–58, 1907*
13. *Li Y X and Xu J L, Nanoscale and Microscale Thermophys. Eng., 10, 109-141, 2006.*
14. *Li Y X and Xu J L, Intl. J. Heat and Mass Trans., 50, 2571-2581, 2007.*